Combust. Sci. and Tech., 179: 1183–1203, 2007
Copyright © Taylor & Francis Group, LLC
ISSN: 0010-2202 print/1563-521X online
DOI: 10.1080/00102200601015574

Taylor & Francis
Taylor & Francis Group

Effects of Moisture on Ignition Behavior of Moist California Chaparral and Utah Leaves

Thomas H. Fletcher,* Brent M. Pickett, Steven G. Smith, Gregory S. Spittle, Megan M. Woodhouse, and Elizabeth Haake
Chemical Engineering Department, Brigham Young University, Provo, Utah

David R. Weise
PSW Research Station, Forest Fire Laboratory, USDA Forest Service, Riverside, California

Abstract: Individual cuttings from eight plant species native to California chaparral or Utah were burned in a well-controlled, well-instrumented facility. Gas temperatures above a flat-flame burner were controlled at 987 ± 12°C and 10 ± 0.5 mol% O_2, resulting in a heat flux at the leaf surface varying from 80–140 kW/m^2. High moisture leaves were observed to burst due to the rapid escape of vapor from the leaf interior. Bubbles in or on the leaf surface were observed for leaves with moderate moisture contents. A large number of leaf temperature measurements were made, along with measurements of the ignition time and temperature, flame height, and flame duration. Average ignition temperatures were species dependent, ranging from 227°C to 453°C, with a large degree of scatter from leaf to leaf. Correlations of time to ignition and ignition temperature were made, but showed only a weak dependence on leaf thickness and almost

Received 3 April 2006; accepted 1 September 2006.
This research was funded by the USDA/USDI National Fire Plan administered through a Research Joint Venture Agreement (No. 01-CR-11272166-168) with the Forest Fire Laboratory, Pacific Southwest Research Station, USDA Forest Service, Riverside, CA. Special thanks to Joey Chong from the Forest Fire Laboratory, who helped with the collection of chaparral samples. Part of this manuscript was prepared by a U.S. Government employee on official time and with government funding and is therefore in the public domain and not subject to copyright laws.
*Address correspondence to tom_fletcher@byu.edu

no dependence on mass of moisture in the leaf. Leaf samples with similar mass showed that Utah juniper took longer to burn than the other species, and that the Utah broadleaf species burned more rapidly than all the other species.

Keywords: Ignition; Live fuels; Wildland fire

INTRODUCTION

Current wildland fire models in the United States are based on the extensive empirical correlations developed by Rothermel (1972), Van Wagner (1973), Albini (1976), Byram (1959), Fosberg and Deeming (1971), and others. These correlations were normally generated from data on fire spread through beds of wood (*Populus tremuloides* excelsior, *Pinus ponderosa* sticks) or cast foliage (such as needles from various *Pinus* trees). The operational models currently used by fire managers to predict fire spread and danger are FARSITE (Finney, 1998), BEHAVE (Andrews, 1986), and the National Fire Danger Rating System (Deeming et al., 1972) which use these empirical correlations to account for effects of fuel quantity and type, wind, and slope. These models have proven to be accurate for prediction of surface fire spread rates in forests and rangelands under many conditions from which the empirical correlations were developed. More recent models (Linn, 1997) have included sophisticated treatments of fluid dynamics to account for the interaction of the wind and the fire, but have not made improvements in the fuel combustion model. Fire spread rates and intensity in live vegetation are also predicted by these models, but with less accuracy. Porous media models that include some treatment of chemical reactions have also been developed, but have not been widely implemented due to their computational time (Zhou and Pereira, 2000; Morvan and Dupuy, 2004; Dold et al., 2005; Zhou et al., 2005).

Combustion data for live vegetation must be obtained in order to improve current wildland fire models, especially when trying to predict when fires move from the ground to the tree crowns and for predicting flare-ups. Differences in the pyrolysis behaviors of 23 species of wildland fuels were investigated by Susott (1982) using evolved gas analysis (EGA). This technique involved shredding the samples in order to focus on chemical effects rather than heat and mass transfer effects. Very little difference was observed in the pyrolysis behavior of leaves of different species, although differences were observed between classes of vegetation, such as between leaves, stems, and bark. Thermal gravimetric analysis (TGA) was also used to study 12 plant species in the Mediterranean (Dimitrakopoulos, 2001); pyrolysis was observed to start between 177 and 228°C and end between 468 and 492°C.

Even though Susott and Dimitrakopoulos observed similar pyrolysis behavior for different leaves in their experiments, these same species exhibit differences in combustion behavior in real fires, such as flame height and extent of brand generation. The lack of variation in the pyrolysis behavior of the live vegetation samples seems to indicate that combustion behavior of live vegetation is limited by the effects of heat and mass transfer. Therefore, in order to understand the differences in live fuel combustion behavior, an apparatus was developed to study the combustion behavior of whole leaf samples. The characterization of this apparatus and the initial data on the combustion behavior of live vegetation were reported by Engstrom et al. (2004). Most of the data collected by Engstrom and coworkers were from samples that had been in the lab for a few weeks, and hence the samples had fairly low moisture contents when burned. These experiments showed effects of shape, vertical vs. horizontal orientation, and leaf thickness on the time to ignition and the temperature at ignition. This paper focuses on using this technique to explore the differences in combustion behavior (qualitative and quantitative) between high moisture (fresh cut) and low moisture leaf samples. Differences are reported as a function of species, leaf thickness, and moisture content.

EXPERIMENTAL MATERIALS

Fire burns living vegetation in many parts of the western United States as well as in the southern U.S. In southern California, wildland fires often occur in chaparral, which is a Spanish word for the shrub vegetation that grows between 700 and 1699 m elevation. Similar vegetation grows in other Mediterranean climates around the world, notably Chile, southern Europe, Australia, and South Africa. In the interior western United States, fires burn in shrub vegetation as well as in coniferous vegetation. Four common chaparral species and four interior western species were selected for testing. The chaparral species used were manzanita (*Arctostaphylos glandulosa*), ceanothus (*Ceanothus crassifolius*), scrub oak (*Quercus berberidifolia*), and chamise (*Adenostoma fasciculatum Hook. & Arn.*). The Utah species used were big sagebrush (*Artemisia tridentata Nutt.*), Gambel oak (*Quercus gambelii Nutt.*), canyon maple (*Acer grandidentatum Nutt.*), and Utah juniper (*Juniperus osteosperma* (*Torr.*) Little). Foliage and branch samples were cut in the field and transported quickly to the laboratory. Samples were sealed and kept cool to minimize moisture loss.

EXPERIMENTAL APPARATUS

The experimental apparatus was described in detail by Engstrom et al. (2004) and is designed to closely resemble the conditions of a wildland flame front. Temperatures in wildland fires are thought to be about 1200 K (Butler et al., 2004), with heating rates of approximately 100 K/s (Butler, 2002). To simulate this condition, the fuel sample was attached to a stationary horizontal rod positioned on a mass balance with a counterweight. A flat-flame burner (FFB) was positioned on a moveable platform to simulate the flame front. The post-flame gases from the FFB heat the suspended leaf by convection. Engstrom and coworkers determined from infrared video images that the optimal location for samples in this experiment was 5 cm above the burner, where the post-flame temperature was 987°C ± 12°C, with about 10 mol% O_2 in the post-flame gases. Previous analysis of the leaf surface temperature histories showed that maximum heat flux on manzanita was approximately 100 kW/m^2 (Engstrom et al., 2004). Other samples experienced similar heat fluxes ranging from 80–140 kW/m^2.

Leaf surface temperature data were obtained at 20 Hz using a type K (chromel-alumel) thermocouple with a bead size of 127 μm diameter. The thermocouple was embedded in a pinhole in the leaf edge near the ignition point for the broadleaf samples. Thermocouple data were not taken for the chamise or juniper samples due to the small dimension of the needles, and due to the movement of these samples during combustion. All of the mass, video, and temperature data were time-stamped for quick and accurate comparison.

A FLIR thermal imaging (IR) camera (model A20M) was also used to measure leaf temperatures in the vicinity of the thermocouple.[1] Figure 1 shows a typical plot of the thermocouple readings compared to the maximum IR temperature near the location of the thermocouple. The thermocouple data correlate well with the IR temperature data using an emissivity (ε) of 0.70–0.85, with the best least squares fit obtained using $\varepsilon = 0.75$.

The types of leaves examined are listed in Table 1 along with key characteristics; additional descriptions are given by Smith (2005). Proximate analyses were performed on dry crushed leaf samples according to the American Society for Testing Materials (ASTM) standards set for coal and coke (Clarence Karr, 1978) (i.e., heating to 950°C in a crucible with a lid to determine volatiles content, burning in an open crucible in air at 750°C for ash content). The ash content varied from approximately 2–5% and volatile matter varied from 74.5–76.9% on a moisture-free basis (see Table 1). Char content in the ASTM test (i.e, the organic residue after devolatilization) was therefore consistently near 20% of the sample on a moisture-free basis. ASTM ultimate analyses were also

[1]Note: The use of trade names is provided for information purposes only and does not constitute endorsement by the U.S. Department of Agriculture.

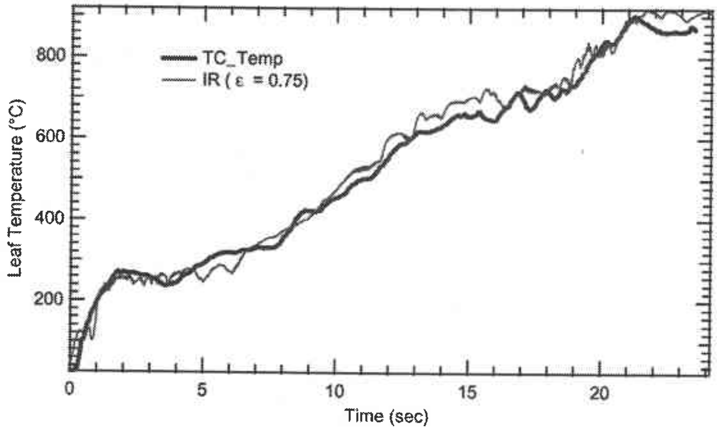

Figure 1. Comparison of type K thermocouple reading to IR temperature reading on a manzanita leaf.

performed and showed similar elemental compositions for each species (see Table 1). Sulfur and other trace elements were neglected from the ultimate analysis, since very small amounts are present in biomass fuels. The similar elemental compositions imply that the heating values are similar. This information supports Susott's (1982) EGA work that indicates different species are made up of similar components (like cellulose and lignin) and behave similarly during pyrolysis.

Moisture contents are reported in Table 1 on an oven-dry weight basis (Babrauskas, 2003), defined as the mass of moisture divided by the mass of dry sample ($m_{moisture}/m_{dry}$), as is customary in the forest products industry. The moisture content analysis was performed using a CompuTrac moisture analyzer on the day of the experiment. Approximately 2 grams of foliage were loaded into the analyzer, heated to 98°C and maintained there until the mass no longer changed mass. Freshly-cut California chaparral samples were sealed and express-mailed to BYU for analysis; moisture content decreased as the sample sat in the laboratory. The moisture content of these fresh samples was as high as 200% on an oven-dry basis (i.e., 67 wt% on a total moist mass basis).

RESULTS AND DISCUSSION

Over 1100 experiments on individual leaf samples were performed over a three-year period. Video images were recorded as well as temperature and mass profiles. The effect of buoyancy on the mass measurements is currently being studied; hence this article focuses on the video images and temperature measurements. All broadleaf data in this article were

Table 1a. Characteristics of California chaparral leaves

Species	Ash content*(%)	Volatile matter content* (%)	Moisture content* (%)	Ultimate analysis† (%)		Leaf thickness (mm)	Leaf length (cm)	Leaf width (cm)
Manzanita *Arctostaphylos glandulosa*	2.2	76.9	45–105	C	52.77	0.15–1	2–4	1.3–2.6
				H	6.32			
				N	0.78			
				O	40.13			
Ceanothus *Ceanothus crassifolius*	3.2	75.8	35–105	C	52.94	0.1–0.9	1–2.4	0.8–1.6
				H	6.30			
				N	1.08			
				O	39.67			
Chamise *Adenostoma fasciculatum Hook. & Am.*	2.8	76.9	75–85	C	51.48	0.5–0.6 (needle diameter)	4–6.5 (sprig length)	0.4–0.6 (needle length)
				H	6.61			
				N	1.31			
				O	40.60			
Scrub Oak *Quercus berberidifolia*	5.1	74.5	45–95	C	51.47	0.15–0.8	2–4.4	1–2.8
				H	6.50			
				N	1.99			
				O	40.03			

*Wt, Dry basis; †Wt, Dry ash free basis.

Table 1b. Characteristics of leaves from Utah foliage

Species	Ash content* (%)	Volatile matter content* (%)	Moisture content* (%)	Ultimate analysis† (%)		Leaf thickness (mm)	Leaf length (cm)	Leaf width (cm)
Gambel Oak *Quercus gambelii Nutt.*	2.9	83.5	50–125	C	49.15	0.1–0.4	3–11	1.5–9
				H	6.23			
				N	2.52			
				O	42.10			
Canyon Maple *Acer grandidentatum Nutt.*	3.5	83.9	55–120	C	45.93	0.1–0.5	2–6	3–8
				H	6.14			
				N	2.11			
				O	45.82			
Utah Juniper *Juniperus osteosperma (Torr.) Little*	4.0	84.8	40–70	C	49.92	1–1.5 (needle diameter)	3.5–8 (sprig length)	0.4–1.0 (needle length)
				H	6.88			
				N	1.33			
				O	41.87			
Big Sagebrush *Artemesia tridentata Nutt.*	3.9	85.2	115–200	C	48.52	0.1–0.5	2–5	0.6–1.2
				H	6.46			
				N	2.25			
				O	42.77			

*Wt, Dry basis; †Wt%, Dry ash free basis.

obtained with the leaf in a horizontal orientation, since that is the way these leaves generally occur in nature. Both qualitative and quantitative results are discussed here. More detail and documentation can be found in Smith (2005) and Pickett (2006).

Qualitative Results

Bubble Formation. One of the most interesting phenomena observed during ignition of broadleaf species was the appearance of bubbles beneath or on top of the upper leaf surface. The leaf samples with the highest moisture contents (generally greater than 80%) exhibited explosive release of moisture, resulting in small craters or pockmarks appearing in the leaf surface. The extent of bubbling or bursting observed was a function of the moisture content of the leaf. For example, manzanita leaves with a 73% moisture content showed bubbles moving around on the surface of the leaf (Figure 2a), while manzanita leaves near 100% moisture content showed bursting (Figures 2b and 2c). A summary of bubbling/bursting phenomena for all species observed is given in Table 2 (see Smith (2005) and Pickett (2006) for more details). The only species that exhibited the bubbles on top of the leaf surface (rather than beneath the leaf surface) was manzanita. No bursting behavior was observed for the thin-leaf samples (canyon maple, big sagebrush, and gambel oak).

The bubbles form as evaporated moisture tries to escape from the interior of the leaf, and the mass transfer of this moisture is limited by pore diffusion or the waxy layer on the leaf surface. The bursting behavior is thought to occur because of the large volume of moisture in the leaf interior, which causes a large internal pressure during evaporation. If the internal pressure overcomes the skin surface tension, bursting occurs. The craters were approximately 6 mm in diameter for the manzanita leaves, which is fairly large compared to the dimensions of the leaves (approximately 35 mm long and 19 mm wide).

To better analyze the bursting characteristics of manzanita leaves, individual leaf samples were subjected to the convective gases of the FFB until bursting was observed, and then were quickly removed from the convective gases. As shown in Figure 2c, the upper epidermis of a manzanita leaf appears to have detached from the main body of the leaf.

There are two ways the vaporized water escapes the leaf interior: (1) through the stomata (small pores on the surface of the leaf allowing moisture transfer into and out of the leaf (Nelson, 2001)) or (2) through the epidermal layers. The path of least resistance is for the moisture to evaporate into the void spaces surrounding the spongy mesophyll cells on the lower interior part of the leaf. From there, the vaporized moisture can either escape through the stomata (usually more numerous on the

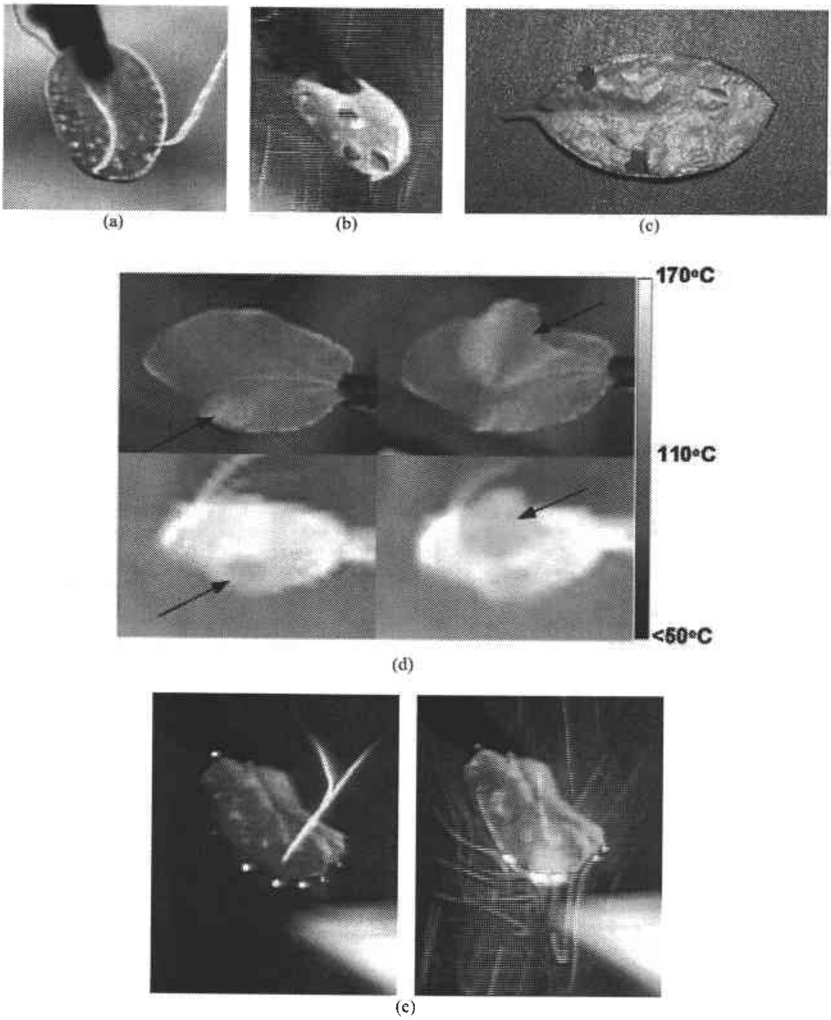

Figure 2. (a) Bubbling manzanita with moisture content of 73%. (b) Bursting manzanita with moisture content near 100% during reaction in FFB. (c) Upper surface of burst manzanita leaf. Sample was removed from FFB after bursting occurred. (d) Video camera images and corresponding IR camera images of a bursting manzanita leaf. The duller yellow spots correspond to the lower temperature of the bursting region. (e) Ignition on the spines of California scrub oak (MC = 79%) followed by explosive expulsion of the spines. (See Color Plate 1 at the end of this issue).

underside of the leaf, sometimes exclusively) or bubble/burst through the lower epidermis. Experiments on scrub oak and ceanothus have shown bubbling/bursting occurs on the under side of the leaf. The upper side

Table 2. Summary of bubbling/bursting phenomena for broadleaf species

Species	Moisture content (%)	Observations
Manzanita	<70	No bubbling
	~75	Bubbles formed on surface prior to ignition
	~100	Bursting behavior prior to ignition
Scrub Oak	~60	Bubbles formed underneath top surface prior to ignition
	~72	Bursting observed on underside of leaf
Ceanothus	~64	Bursting observed on underside of leaf
Gambel Oak	52	Bubbles formed underneath top surface prior to ignition
Canyon Maple	86	Bubbles formed underneath top surface during and after ignition

of the leaf contains columns of organized cells (palisade mesophyll cells) which protects the upper side from bursting. However, manzanita exhibited upper side bursting, suggesting that the layer of palisade cells in the manzanita leaves is not as organized as in the scrub oak and ceanothus.

A hissing noise was observed when scrub oak leaves were burned right side up, suggesting that the vapor inside the leaf could not exit through the stoma quickly enough. However, when the leaves were burned upside down, little or no hissing was observed, indicating that the vapor was exiting through the more numerous stomata located on the underside of the leaf (i.e., the top of an upside-down leaf). If the leaf heats up faster than the moisture can diffuse through the epidermal layer or out the stomata, then the pressure will build up inside the leaf until it exceeds the surface tension of the leaf, which causes moisture to be released by interior bubbling or bursting through the leaf surface. Bursting may occur at multiple stomata or at multiple locations of the epidermis, leading to pockmarks as seen in Figures 2b and 2c. Figure 2d shows video camera images and corresponding IR camera images of a bursting manzanita leaf. When the IR image of the manzanita leaf was analyzed (assuming an emissivity of 0.75), a temperature drop of about 40°C was observed at the location of the burst over a period of 0.10 seconds (Figure 2d). It is believed that this local temperature drop on the leaf surface is due to evaporated water escaping from the hot pocket inside the leaf surface following the burst.

Ignition Behavior. Both the low and high moisture manzanita samples in the horizontal orientation ignited almost uniformly around the leaf perimeter before burning in towards the center of the leaf, as discussed by Engstrom et al. (2004). This was the general behavior of most of the other broadleaf samples as well when samples had no points or spines. In contrast, many of the scrub oak leaves had sharp points (i.e., spines) around the outer edge. The high moisture scrub oak leaves ($\sim$80%) would ignite at these spines, sometimes accompanied by small explosions of the points that led to the ejection of small brands (see Figure 2e). The ignition at the points was followed by ignition along the entire perimeter, followed by burning towards the center of the leaf. In contrast, the lower moisture samples exhibited ignition at the perimeter with little or no expulsion of tiny embers from the spines.

A unique behavior was also observed for the sagebrush leaves. Fresh sagebrush samples exhibited a high moisture content, often near 150%. The sagebrush leaves were less rigid (i.e., more pliable) than the other leaf samples. Although high in moisture content, sagebrush was fairly quick to ignite (quicker than manzanita or ceanothus). Ignition would usually first occur on the tip of one or more of the three lobes. Not long after ignition, the opposite end of the leaf would ignite near the stem of the leaf, followed by engulfing flames over the entire leaf. The early burning of the stem caused the leaf to break away from the clip before significant burnout, generating brands approximately the size of the leaf.

Samples with needles (chamise and juniper) ignited on the tips of the needles, and then individual flames coalesced into one large flame as combustion proceeded. Small brands of the chamise were formed as combustion of the stem occurred, breaking the twig into several pieces (Smith, 2005). This brand formation behavior was not noted for the juniper samples, but the berries on the juniper burned longer, which subsequently formed brands.

A color change in the leaf was observed prior to ignition in many of the broadleaf samples. For example, manzanita leaves turned a dusty green to a wet green prior to ignition. Scrub oak leaves became very shiny and started to curl just prior to ignition. Color change was not observed for the juniper needles, but a wax-like substance was observed to seep out of the juniper needles and drip onto the FFB during heating and ignition.

The video and infrared images have shown interesting qualitative differences in the combustion behavior of these leaf samples. A summary of many of the observed surface phenomena for manzanita samples is shown in Figure 3, superimposed on an actual manzanita leaf temperature profile. Similar qualitative behavior occurred in other species, although it is likely that the observed phenomena overlap in different samples. For example, bubbling may overlap with ignition and sometimes even start after ignition.

Quantitative Results

Ignition. Preliminary data regarding ignition temperature (T_{ig}) and time to ignition (t_{ig}) were gathered for low moisture samples of manzanita, scrub

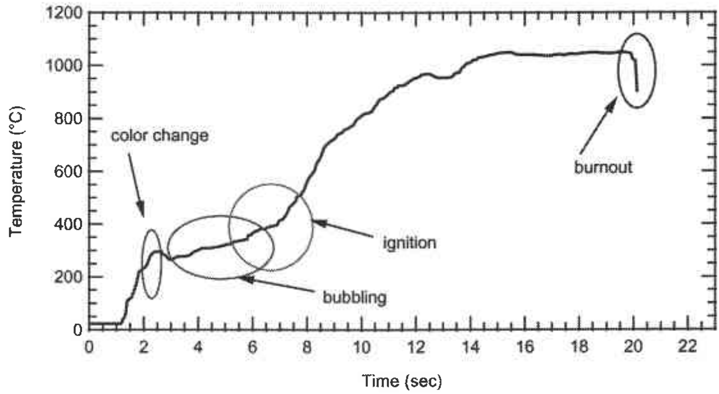

Figure 3. Representative temperature curve showing the observed surface phenomena for a manzanita sample with a moisture content of 73%.

oak, and ceanothus by Engstrom et al. (2004). In these experiments, ignition temperature was defined as the temperature at the time when a sustainable flame was first visible after frame-by-frame inspection of the video images. The time stamp on the video frame was used to determine the corresponding temperature from the thermocouple measurement.

Figure 4 shows the average T_{ig} for each species in decreasing order, with corresponding values of t_{ig}, along with the 95% confidence values as error bars. The average ignition temperatures ranged from 227°C for gambel oak up to 453°C for ceanothus. It is interesting to note that the

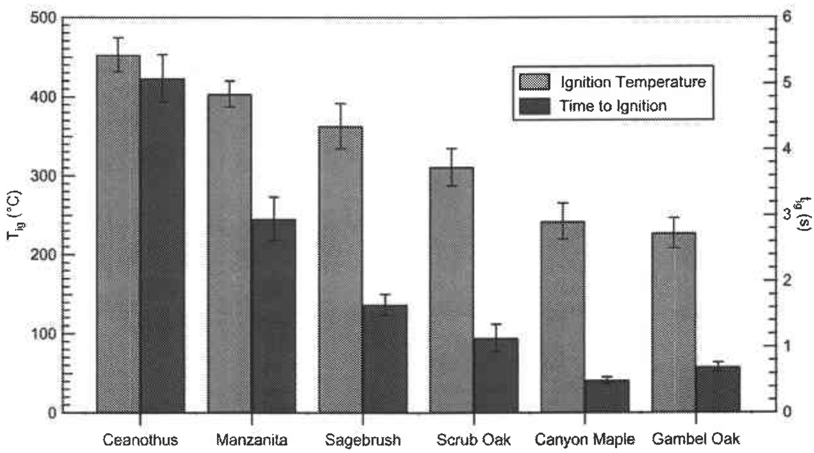

Figure 4. Average measured values of T_{ig} and t_{ig} for California chaparral and Utah broadleaf species. The error bars represent the 95% confidence interval for these data.

average t_{ig} follows the decreasing trend of T_{ig} except for canyon maple. Canyon maple has a larger perimeter with sharper points than other species studied, which could cause it to ignite earlier than other species. There is a large degree of scatter in the measured values of T_{ig}, as reflected in the large values of the standard deviations in T_{ig} (Pickett, 2006), which ranged from 109 to 159°C. The standard deviations in t_{ig} (Pickett, 2006) also vary widely, from 0.24 s for canyon maple to 2.33 s for manzanita.

The values of T_{ig} and t_{ig} shown in Figure 4 are the average values for all samples of each species, regardless of other effects such as leaf thickness and/or moisture content. The large amount of scatter in the data made it difficult to give a definitive correlation on T_{ig} and t_{ig}. Many different attempts to correlate the data were made (thickness, moisture content, mass of moisture in sample) to reduce the amount of scatter (Smith, 2005). Correlations using only moisture and not thickness resulted in linear correlations with errors in the slope that were greater than the slope itself. Correlations with thickness showed the most promise (see Figures 5 and 6). As thickness was increased, which varies by a factor of almost 10 (0.1 mm to 0.95 mm), both T_{ig} and t_{ig} appeared to increase, especially for the scrub oak. Babrauskas (2003) states that a linear relationship between t_{ig} and thickness indicates thermally-thin behavior (i.e., small internal temperature gradients), and cites linear results for ignition tests performed in a furnace at 750°C on 3 cm by 1 cm samples cut from dry leaves (Montgomery and Cheo, 1971).

Moghtaderi et al. (1997) observed an increase in T_{ig} at higher moisture content in wood samples. Dimitrakopoulos and Papaioannou (2001) observed an increase in t_{ig} at higher moisture levels for leaf samples. Some of the scatter is likely caused by variability in the moisture of the leaf. Attempts were made to correlate T_{ig} and t_{ig} as a function of thickness and either moisture content (MC, on a dry basis) or mass of moisture per leaf (m_{H_2O}, to account for the leaf-to-leaf variation in mass). Leaf thickness and m_{H_2O} for a given species seemed to follow some pattern (see Figure 7), although two lobes of correlation were apparent for two species (scrub oak and canyon maple). A combined correlation (Smith, 2005) of m_{H2O} and thickness was made for both T_{ig} and t_{ig}, with the goal of finding a simple correlation to use with current firespread models. This correlation was made using the following equations:

$$T_{ig} = a \cdot \Delta x + b \cdot m_{H_2O} + c \tag{1}$$

$$t_{ig} = d \cdot \Delta x + e \cdot \Delta H_{vap} \cdot m_{H_2O} \tag{2}$$

where *a*, *b*, *c*, *d*, and *e* are species-specific constants, Δx is the leaf thickness (mm), ΔH_{vap} is the heat of vaporization for water (2256.9 kJ/kg), and m_{H_2O} is the mass of the moisture (gm). Results of the correlation are shown in Table 3.

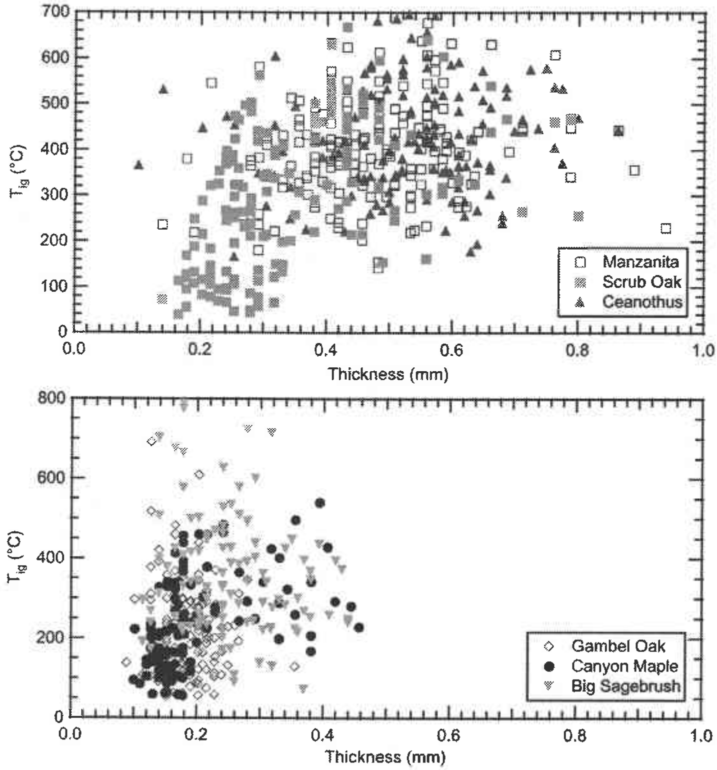

Figure 5. T_{ig} vs. leaf thickness for (a) California chaparral species and (b) Utah species.

The large 95% confidence intervals on the coefficients of the T_{ig} correlation shown in Table 3 indicate that use of these variables (Δx and m_{H_2O}) does not reduce the large scatter in the T_{ig} data. The negative *b* coefficient indicates that moisture has a decreasing effect on T_{ig} for all species except gambel oak. However, since the confidence intervals are greater than the *b* coefficients, the *b* coefficients are not significantly different than zero (except for canyon maple). In addition, the magnitude of m_{H_2O} is small (~1–10 mg), so that even the largest moisture-related coefficients in Table 3 have a small effect.

The thickness coefficients (*d*) for fitting t_{ig} are clearly positive for all species. In contrast, the m_{H_2O} coefficient (*e*) is positive for some species (ceanothus, gambel oak, and sagebrush), essentially zero for others (manzanita and canyon maple), and slightly negative for scrub oak. However, the large confidence intervals for the scrub oak coefficient (*e*) indicate that these decreasing effects may not actually occur.

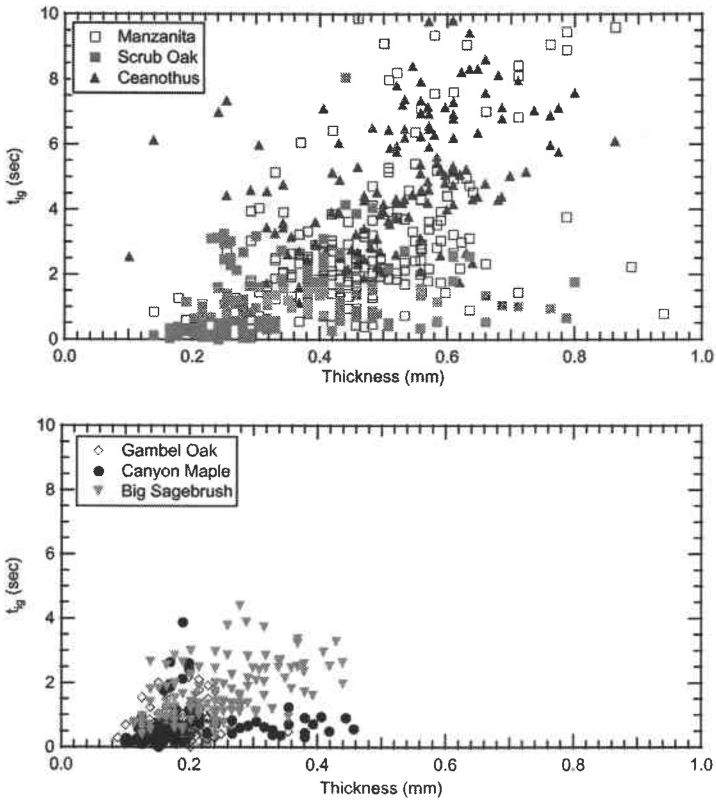

Figure 6. t_{ig} vs. leaf thickness for (a) California chaparral species and (b) Utah species.

The large uncertainty in the coefficients for the T_{ig} correlation in Table 3 raises the question of the benefit of the correlation above and beyond using the mean value of T_{ig}. This was checked by comparing the sum-square error (SSE) by (1) using the correlation and (2) using the mean value. For three species (ceanothus, gambel oak, and sagebrush) the mean value only raised the SSE by less than 7%, while the SSE was raised 18%, 28%, and 32% for manzanita, scrub oak, and canyon maple, respectively. This means that the use of the mean value of T_{ig} is almost as good as using the correlation for these species. Ceanothus was the only species where the SSE for the correlation of t_{ig} was significantly greater (by a factor of $\sim$2) than that for the average value of t_{ig}. These results indicate that leaf thickness had only a slight influence on the measured values of T_{ig} and t_{ig}, and that the mass of moisture had an even smaller effect.

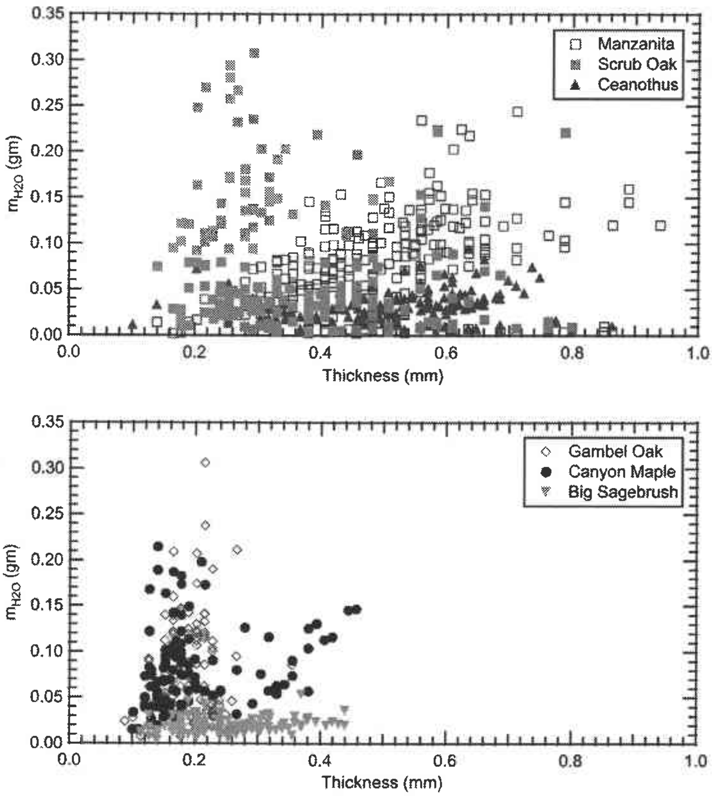

Figure 7. Mass of moisture per leaf (m_{H_2O}) versus thickness for (a) California chaparral and (b) Utah samples.

Table 3. Coefficients used in predicting T_{ig} from Equations 1 and 2 for the different species

Species	T_{ig} (°C)			t_{ig} (sec)	
	a	*b*	*c*	*d*	*e*
Manzanita	387 ± 223	−27 ± 496	221 ± 85	5.2 ± 1.35	1.55 ± 2.9
Scrub Oak	526 ± 174	−219 ± 346	144 ± 73	3.01 ± 0.46	−0.64 ± 0.72
Ceanothus	157 ± 180	−296 ± 1340	401 ± 98	6.1 ± 0.95	29.9 ± 6.43
Gambel Oak	−858 ± 685	353 ± 446	359 ± 120	1.97 ± 0.81	1.68 ± 0.68
Canyon Maple	424 ± 269	−940 ± 554	270 ± 82	1.91 ± 0.44	0.33 ± 0.46
Sagebrush	83 ± 562	−2715 ± 4250	414 ± 142	3.61 ± 1.49	15.9 ± 8.1

*The ± represents 95% confidence interval for these coefficients.

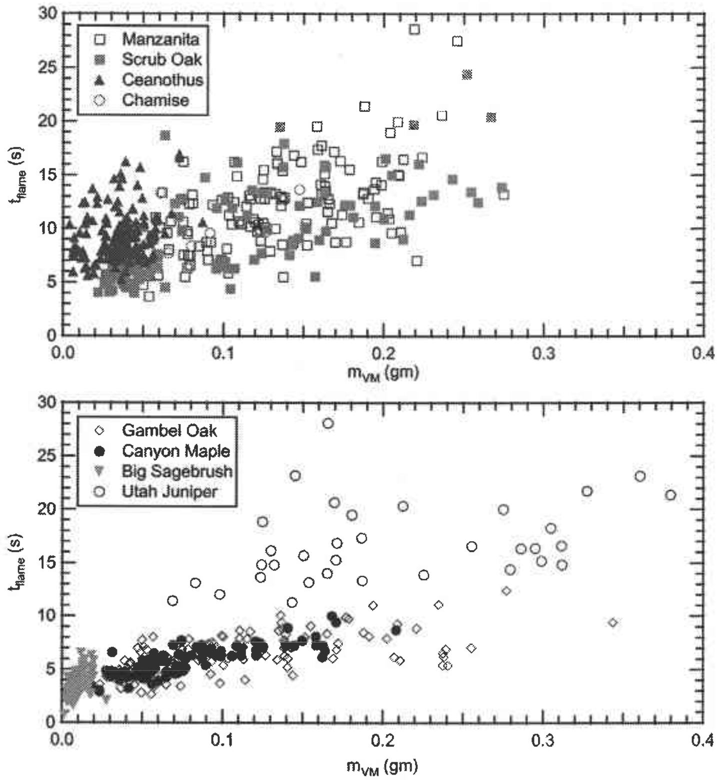

Figure 8. Burnout time (t_{flame}) vs mass of volatiles (m_{VM}) for (a) California chaparral and (b) Utah species.

An examination of the measured temperature profiles, both with the embedded thermocouple and with the infrared camera, showed that the profile for most broadleaf species was similar to the profile shown earlier in Figure 1. It is interesting to note that the measured profiles do not show a plateau at 100°C (i.e., the boiling point of water), or at a temperature that would be indicative of a specific pyrolysis temperature. The weak plateau observed in Figure 1 at 250°C was observed in most of the other measured temperature profiles at temperatures ranging from 250°C to 350°C. This lack of a plateau at 100°C is likely due to the two-dimensional nature of leaf combustion and the complicated mass and heat transfer involved inside and around the leaf.

Burnout Time. The burnout time (t_{flame}) was defined as the amount of time that the flame was visible in the video images. Burnout time was

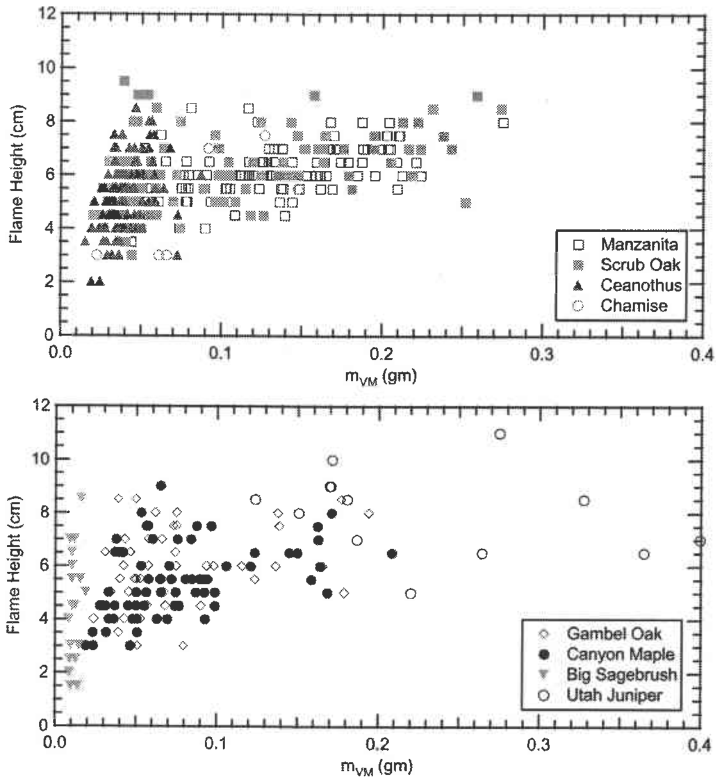

Figure 9. Estimated maximum flame height vs. initial volatile mass for (a) California chaparral and (b) Utah species.

expected to correlate with the amount of fuel available, and is roughly related to reaction rate if the mass of the remaining charred leaf is small. Figure 8 shows the burnout time observed for the chaparral and Utah species versus the amount of volatile mass of the sample (m_{VM}). It is clear that the burning time for the Utah Juniper is about 10 s longer than for the other Utah species of the same volatile mass. The burning times for all of the other three Utah broadleaf species examined fell along the same line in this plot (Figure 8b). The t_{flame} data for each chaparral species showed more scatter than the Utah species, but only the ceanothus seemed to show a slightly larger flame duration at a given initial volatile mass than the other three California species. The California chaparral data in Figure 8 spanned a larger range of moisture contents than the Utah samples, which may account for the larger degree of scatter. It is also interesting to note that the flame duration for the three broadleaf Utah species (gambel oak, canyon maple, and big sagebrush) was less than that observed for the California chaparral species of similar initial volatile mass.

Flame Height. The maximum flame height for each sample was determined from visual inspection of the video images. It was expected that the flame height of the sample would also correlate with the initial amount of volatile mass available (m_{VM}) or with the leaf reaction rate (dm/dt). Others have correlated flame height with heat release rate (Hasemi and Takunaga, 1989; Drysdale, 2002), which is related to the mass release rate if the heats of combustion are similar. The flame height of the sample reaches a maximum between ignition and burnout, usually around 2/3 of the time through the flaming period. For each individual run, all the video frames were analyzed, and the estimated maximum flame height and time were recorded. This flame height was estimated (±0.5 cm accuracy) using the thickness of the alligator clip as a reference.

The recorded flame height is compared with the volatile mass in Figure 9. The flame heights for these experiments ranged from about 2 to 10 cm. There was a slight increase in flame height with increase in initial volatile mass for all species.

CONCLUSIONS

Experiments were performed to study the combustion behavior of 8 live fuels, focusing on the effects of size, shape, and moisture. Qualitative experiments have shown that combustion behavior varies according to species. Small bubbles formed on and inside broadleaf samples at moderate moisture content (~70% on an oven-dry basis). Small craters formed on broadleaf chaparral species at high moisture content (80–110%). Small brands were also uniquely formed, depending on species.

Average ignition temperatures of different species varied from 227°C to 453°C, and the average time to ignition varied from 0.5 s to 5.1 s, with large amounts of scatter. Attempts were made to reduce the scatter in the ignition temperature and time to ignition data by correlating with leaf thickness and/or the mass of moisture per leaf; these correlations showed a weak dependence on leaf thickness and no independent effect of the mass of moisture. The leaf temperature profiles did not show a plateau at 100°C, regardless of moisture content; a plateau was observed in some temperature profiles at about 275°C, which does not agree with conceptual models.

These experiments show promise for understanding the details of the ignition and combustion processes for leaves in a wildland fire environment. The qualitative and quantitative data from this experiment should prove valuable in developing correlations to improve descriptions of combustion behavior in wildland fire models.

REFERENCES

Albini, F.A. (1976) Estimating Wildfire Behavior and Effects INT-30, USDA Forest Service.

Andrews, P.L. (1986) BEHAVE: Fire Behavior Prediction and Fuel Modeling System- BURN Subsystem, Part 1 INT-**194**, USDA Forest Service.

Babrauskas, V. (2003) Ignition Handbook, Fire Science Publishers, Issaquah, WA.

Butler, B.W. (2002) Personal communication.

Butler, B.W., Finney, M.A., Andrews, P.L., and Albini, F.A. (2004) A radiation-driven model for crown fire spread. *Can. J. Forest Res.*, **34**(8), 1588–1599.

Byram, G.M. (1959) Combustion of forest fuels. In Davis, K.P. (Ed.) *Forest Fire: Control and Use*, McGraw-Hill, New York, pp. 61–89.

Clarence Karr, J. Ed. (1978). *Analytical Methods for Coal and Coal Products*, Academic Press, Inc., New York.

Deeming, J.E., Lancaster, J.W., Fosberg, M.A., Furman, R.W., and Schroeder, M.J. (1972) National Fire-Danger Rating System. *USDA Forest Service Research Paper*, RM-84, Ft. Collins, CO.

Dimitrakopoulos, A.P. (2001) Thermogravimetric analysis of mediterranean plant species. *J. Anal. Appl. Pyrolysis*, **60**, 123–130.

Dimitrakopoulos, A.P. and Papaioannou, K.K. (2001) Flammability assessment of mediterranean forest fuels. *Fire Technol.*, **37**(2), 143–152.

Dold, J., Greenberg, J.B., Weber, R., Zinovlev, A. and Sivashinsky, G. (2005) A porous-medium model for vegetation in bushfires. Fifth Asia-Pacific Conference on Combustion, Adelaide, Australia.

Drysdale, D. (2002) An Introduction to Fire Dynamics, John Wiley & Sons, New York.

Engstrom, J.D., Butler, J.K., Smith, S.G., Baxter, L.L., Fletcher, T.H., and Weise, D.R. (2004) Ignition behavior of live california chapparal leaves. *Combust. Sci. Technol.*, **176**, 1577–1591.

Finney, M.A. FARSITE: Fire Area Simulator-Model Development and Evaluation, RMRS-RP-4 (1998), USDA Forest Service.

Fosberg, M.A. and Deeming, J.E. (1971) Derivation of the 1- and 10-hour timelag fuel moisture calculations for fire danger rating. Research Note RM-207, Fort Collins, CO, USDA Forest Service.

Hasemi, Y. and Takunaga, T. (1989) Fuel shape effect on the deterministic properties of turbulent diffusion flames. Proceedings of the 2nd International Symposium on Fire Safety Science, 275–286.

Linn, R.R. (1997) A Transport Model for Prediction of Wildfire Behavior, Mechanical Engineering, New Mexico State University, Las Cruces, NM.

Moghtaderi, B., Novozhilov, V., Fletcher, D.F., and Kent, J.H. (1997) A new correlation for bench-scale piloted ignition data of wood. *Fire Safety J.*, **29**, 41–59.

Montgomery, K.R. and Cheo, P.C. (1971) Effect of leaf thickness on ignitability. *Forest Sci.*, **17**(4), 475–478.

Morvan, D. and Dupuy, J.L. (2004) Modeling the propagation of a wildfire through a mediterranean shrub using a multiphase formulation. *Combust. Flame*, **138**, 199–210.

Nelson, R.M., Jr. (2001) Water relations of forest fuels. In Johnson, E.A. and Miyanishi, K. (Eds.) *Forest Fires: Behavior and Ecological Effects*, Academic Press, San Diego, pp. 79–143.
Pickett, B. (in progress, 2007) Effects of Moisture on Ignition Behavior of Live California Chaparral and Utah Leaves. Chemical Engineering, Brigham Young University, Provo, Utah.
Rothermel, R.C. (1972) A Mathematical Model for Predicting Fire Spread in Wildland Fuels, INT-115, USDA Forest Service.
Smith, S.G. (2005) Effects of Moisture on Combustion Characteristics of Live California Chaparral and Utah Foliage. Chemical Engineering Department, Brigham Young University.
Susott, R.A. (1982) Characterization of the thermal properties of forest fuels by combustible gas analysis. *Forest Sci.*, **2**, 404–420.
Van Wagner, C.E. (1973) Height of crown scorch in forest fires. *Can. J. Forest Res.*, **3**, 373–378.
Zhou, X., Mahalingam, S., and Weise, D.R. (2005) Modeling of marginal burning state of fire spread in live chaparral shrub fuel bed. *Combust. Flame*, **143**, 183–198.
Zhou, X.Y. and Pereira, J.C.F. (2000) A multidimensional model for simulating vegetation fire spread using a porous media sub-model. *Fire Mater.*, **24**, 37–43.